Geosci. Model Dev. Discuss., 7, 7693–7731, 2014
www.geosci-model-dev-discuss.net/7/7693/2014/
doi:10.5194/gmdd-7-7693-2014

Geoscientific Model Development Discussions
Open Access

Aerosol specification in single-column CAM5

B. Lebassi-Habtezion and P. Caldwell

Livermore National Laboratory, PCMDI, Cloud Processes Research (CPR) Group, Livermore, CA, USA

Received: 14 October 2014 – Accepted: 21 October 2014 – Published: 17 November 2014

Correspondence to: B. Lebassi-Habtezion (habtezion1@llnl.gov)

Published by Copernicus Publications on behalf of the European Geosciences Union.

Abstract

The ability to run a global climate model in single-column mode is very useful for testing model improvements because single-column models (SCMs) are inexpensive to run and easy to interpret. A major breakthrough in Version 5 of the Community Atmosphere Model (CAM5) is the inclusion of prognostic aerosol. Unfortunately, this improvement was not coordinated with the SCM version of CAM5 and as a result CAM5-SCM initializes aerosols to zero.

In this study we explore the impact of running CAM5-SCM with aerosol initialized to zero (hereafter named Default) and test three potential fixes. The first fix is to use CAM5's prescribed aerosol capability, which specifies aerosols at monthly climatological values. The second method is to prescribe aerosols at observed values. The third approach is to fix droplet and ice crystal numbers at prescribed values. We test our fixes in four different cloud regimes to ensure representativeness: subtropical drizzling stratocumulus (based on the DYCOMS RF02 case study), mixed-phase Arctic stratocumulus (using the MPACE-B case study), tropical shallow convection (using the RICO case study), and summertime mid-latitude continental convection (using the ARM95 case study).

Stratiform cloud cases (DYCOMS RF02 and MPACE-B) were found to have a strong dependence on aerosol concentration, while convective cases (RICO and ARM95) were relatively insensitive to aerosol specification. This is perhaps expected because convective schemes in CAM5 do not currently use aerosol information. Adequate liquid water content in the MPACE-B case was only maintained when ice crystal number concentration was specified because the Meyers et al. (1992) deposition/condensation ice nucleation scheme used by CAM5 greatly overpredicts ice nucleation rates, causing clouds to rapidly glaciate. Surprisingly, predicted droplet concentrations for the ARM95 region in both SCM and global runs were around 25 cm^{-3}, which is much lower than observed. This finding suggests that CAM5 has problems capturing aerosol effects in this climate regime.

GMDD
7, 7693–7731, 2014

B. Lebassi-Habtezion and P. Caldwell

1 Introduction

The Single Column Model (SCM) version of Community Atmospheric Model (CAM) is a very important tool efficient development of model numerics and physics. Based on observed test cases, many SCM intercomparison studies of stratocumulus and cumulus cloud-top boundary layers have been undertaken with the goal of improving physical parameterizations of clouds and cloud-related processes and their interactions. A number of SCM intercomparison studies by the Global Energy and Water Experiment (GEWEX) Cloud Systems Study (GCSS) Boundary Layer Cloud Working Group (BLCWG) have been conducted to understand common biases in climate models. For example, one of the early SCM intercomparison studies (Moeng et al., 1996) simulated nocturnal non-precipitating stratocumulus clouds and showed that the LWP decreased substantially during the initial period of the simulation, which was explained by excessive dry air entrainment. Another SCM intercomparison simulations of the Second Dynamics and Chemistry of the Marine Stratocumulus field study (DYCOMS II) research flight RF01 (DYCOMSRF01) also showed low liquid water path (LWP) despite improvement of entrainment rates in the models (Zhu et al., 2005). SCM intercomparison of drizzling stratocumulus from the DYCOMS II research flight 02 (DYCOMSRF02) by vanZanten and Stevens (2005) tested the impact of drizzle in SCMs and found that drizzle decreased LWP substantially in most of the models. Another SCM study by Wyant et al. (2007) also carried out SCM intercomparison simulations for the DYCOMSRF02 case. They found that models need improvement in drizzle, sedimentation, and sub-cloud evaporation parameterizations. A recent SCM and cloud- resolving model intercomparison study by Klein et al. (2009) simulated the mixed-phase stratocumulus cloud observed during the Atmospheric Radiation Measurement (ARM) program's Mixed-Phase Arctic Cloud Experiment (MPACE-B). They found that models generally showed ice water path (IWP) in good agreement with observations while LWP was severely under predicted. This was attributed to the interaction between liquid and ice-phase microphysics suggesting the need to improve the representation of mixed-phase microphysics. Previous SCM and LES intercomparison studies were also undertaken for deep (ARM southern Great Plain (ARM SGP) site) and shallow (Rain in Cumulus over the Ocean (RICO)) convective cases. Ghan et al. (2000) performed an SCM intercomparison study for ARM SGP using eleven SCMs and found that no individual models stood out as superior, and the model ensemble showed close agreement with observations. A recent study by VanZanten et al. (2011) used twelve LES simulations to study the interplay between micro and macro physics processes in the evolution of clouds and precipitation, with a wide range of microphysical representations, during the undisturbed period of the RICO field study. Many features of their LES simulations generally agreed with observations. Similar thermodynamic and energetic behavior was produced as compared to previous studies based on SCMs.

A significant fraction of the uncertainties in climate projections results from the representation of aerosol (Houghton et al., 1996; Haywood and Boucher, 2000; Forster et al., 2007). Aerosols affect climate by directly absorbing and reflecting atmospheric radiation (known as the direct effect) and by changing cloud optical properties and lifetimes (known as aerosol indirect effects). As a result, development and testing of aerosol parameterizations have been a high priority in the climate modeling community.

The inclusion of the prognostic aerosol model in CAM had been a major breakthrough in its development (Abdul-Razzak and Ghan, 2000; Liu et al., 2012). However, CAM5-SCM has not been updated appropriately to handle the addition of prognostic aerosol in CAM. In particular, it initializes aerosol mass mixing ratios to zero. As a result, the default SCM release substantially underestimates IWP and LWP of the SCM simulations for a variety of cloud regimes.

In this study we test the impact of the zero aerosol initialization problem, and we introduce fixes for this issue. To ensure representativeness, we test SCM simulations for a variety of cloud regimes. The SCM cases used for this study include summertime mid-latitude continental convection (ARM95), shallow convection (RICO), subtropical drizzling stratocumulus (DYCOMSRF02), and multi-level Arctic clouds (MPACE-B). Results are analyzed and compared to observations and previous LES results.

GMDD
7, 7693–7731, 2014

2 Methods

2.1 SCAM5 setup

In this study we employed the SCM version of CAM5 (SCAM5), which consists of physics parameterizations driven by prescribed advective tendencies (Hack and Pedretti, 2000).

There are two types of clouds in SCAM5: stratus clouds with symmetric turbulent properties and cumulus clouds with vertically stretched shapes and asymmetric turbulence properties. We use the Morrison and Gettelman stratiform cloud microphysics scheme (Morrison and Gettelman, 2008) and the Park et al. (2014) macrophysics scheme to model stratiform clouds. Deep convection is handled by the modified Zhang–McFarlane parameterization scheme (Zhang and McFarlane, 1995), and shallow convection is parameterized by the University of Washington shallow convection parameterization scheme (Park and Bretherton, 2009). Turbulence is handled following Brethorton and Park (2009). Radiation is calculated using the Rapid Radiative Transfer Model (RRTMG) radiation scheme (Mlawer et al., 1997).

CAM5 is the first version of CAM that was designed to simulate aerosol-cloud interactions. It has a three mode simplified modal aerosol model (MAM3) (Easter et al., 2004; Ghan et al., 2012) with Accumulation, Aitken, and Coarse modes. MAM3 is capable of treating complex aerosol physical, optical, and chemical processes and simulating aerosol size, mass and number distributions. The aerosol size distribution is lognormal, and internal and external mixing between aerosol components is assumed in the model. As mentioned previously, this prognostic aerosol model in SCAM5 mode initializes the mass-mixing ratio of the different aerosol species to zero. Hence we test other fixes to solve this problem as described below.

1. The first method we employed is to fix cloud droplet (N_d) and ice crystal (N_i) concentration (hereafter called FixHydro). This case is the setup in default SCAM5 with prognostic MAM3 but N_d and N_i values are prescribed before the

microphysics call. We then set N_d and N_i tendencies inside the microphysics to zero, which keeps the value of N_d and N_i to their corresponding prescribed values.

2. The second method (hereafter called PrescAero) uses the new prescribed aerosol capability included in Community Earth System Model (CESM) version 1.2. PrescAero prescribes mass mixing ratios of aerosol species using mean climatological values for each month of the year and for each grid cell (based on results from a long prognostic aerosol run). By default prescribed aerosol values are actually specified by daily random draws from a lognormal distribution centered on climatological average values. We turn this random sampling off for SCAM5 because this sampling makes SCAM runs irreproducible and provides occasionally odd values. Random sampling is not needed in the tropics, but may be required to reproduce CAM5 polar climate, in which case ensembles of SCAM5 runs are probably needed.

3. The last method we employed is the observed aerosol case where we use observed mixing ratios and size distributions of the aerosols in MAM3. This method (hereafter named obsAero) modifies the PrescAero methodology to instead use observed mass mixing ratios of the different aerosol species for all the modes. To use this mode, observed values are needed for parameters N_j, $a_{\mathrm{m}j}$, and σ_j for the multimode lognormal aerosol size distribution given by the following equation (Abdul-Razzak and Ghan, 2000):

$$\frac{\mathrm{d}n}{\mathrm{d}a} = \sum_{j=1}^{I} \frac{N_j}{\sqrt{2\pi}\sigma_j} \exp\left\{ -\frac{\ln^2\left(\frac{a}{a_{\mathrm{m}j}}\right)}{2\ln^2\sigma_j} \right\}, \tag{1}$$

where N_j, $a_{\mathrm{m}j}$, and σ_j are the number concentrations of the aerosol mode, the geometric mean dry radius, and the geometric standard deviation of aerosol mode j, respectively.

GMDD
7, 7693–7731, 2014

B. Lebassi-Habtezion and P. Caldwell

2.2 SCAM cases

In an attempt to test aerosol effects over the full range of cloud types, we tested our fixes using case studies from four different cloud regimes. We set up four SCAM5 case simulations using the Default configuration and each of the three different fixes discussed in the previous section. The idealization and setup of each case is based on several SCM and LES intercomparison studies conducted for each of the four different cloud regimes. The details of the experiments conducted are summarized below.

a. a.DYCOMS RF02 case

On 11 July 1999, DYCOMSRF02 sampled drizzling stratocumulus off the coast of California. Measurements from this flight formed the basis for large eddy simulation (LES) and SCM intercomparisons by Ackerman et al. (2009) and Wyant et al. (2007), respectively. For this paper we used an experimental configuration similar to Wyant et al. (2007). Subtropical stratocumulus are important because of all cloud types they have the biggest impact on the planetary radiation budget (Hartmann et al., 1992), and difficulty in simulating them is the leading source of uncertainty in climate sensitivity (Bony and Dufresne, 2005).

Like Wyant et al. (2007), for maintaining an approximate balance between radiative cooling and subsidence warming above the inversion, a constant divergence with a value $3.75 \times 10^{-6}\,\mathrm{s}^{-1}$ was used to create an omega profile in the DYCOMSRF02 case, the RRMTG shortwave radiation was turned off, and we ran our simulations for 6 h. Constant surface latent and sensible heat flux values of 93 and $16\,\mathrm{W\,m^{-2}}$ (respectively) were imposed based on observed mean values from vanZanten and Stevens (2005).

Unlike Wyant et al. (2007), the default RRMTG longwave radiation code was used instead of applying an idealized radiation scheme. We also kept u and v for our simulations constant. Cloud processes were turned off above 700 hPa in order to

Discussion Paper | Discussion Paper | Discussion Paper | Discussion Paper |

GMDD

7, 7693–7731, 2014

Aerosol specification in single-column CAM5

B. Lebassi-Habtezion and P. Caldwell

prevent ice formation at the troposphere, which occurs due to assumptions related to subgrid relative humidity variability in CAM5.

For the FixHydro case, an observed N_d value of 55 cm^{-3} was used as recommended by Wyant et al. (2007). The bimodal lognormal distribution (Eq. 1) was assumed to consist of sulfate aerosols with dry density 1.77 g cm^{-3}. The total number, mode radius, and geometric standard deviation for the aitken (125 cm^{-3}, 0.011 µm, 1.2) and accumulation (65 cm^{-3}, 0.06 µm, 1.7) modes, respectively were used. These values were chosen by Ackerman et al. (2009) to produce an in-cloud droplet concentration in their LES, which matched the observed droplet concentration value of 55 cm^{-3}.

b. b.MPACE-B case

The second case is MPACE-B, which consists of mixed-phase stratocumulus over open Ocean near Barrow, AK. The MPACE-B case is based on Arctic stratocumulus observed during the Mixed-Phase Arctic Cloud Experiment period B, which was the subject of an intercomparison by Klein et al. (2009). The case focused on the period 9 October, 17:00 UTC to 10 October, 05:00 UTC, 2004. This case is useful because it is relatively simple yet includes both liquid and ice processes. The setup of this case was similar to that of Klein et al. (2009). Above 700 hPa, all variables were kept near to their initial values by nudging temperature and moisture with a time scale of 1 h. While Klein et al. (2009) nudged u and v below 700 hPa, values u and v were kept constant at the observed values of -13 m s^{-1} and -3 m s^{-1} (respectively) in our study. Surface latent and sensible heat flux values of 107.7 and 136.5 W m^{-2}, respectively, were used and were kept constant throughout the simulation period. Klein et al. (2009) specified a vertical velocity pressure (omega) value greater then zero at the top of the atmosphere (TOA), which causes huge advective heating from the top of the model, causing the model to crash in a few time steps. For this study we replaced the omega values from Klein et al. (2009) above 500 hPa with values that exponentially decrease

GMDD
7, 7693–7731, 2014

to zero at TOA. The value used for advective temperature (moisture) tendency at the surface is $-4.63 \times 10^{-5}\,\mathrm{K\,s^{-1}}$ ($-3.47 \times 10^{-8}\,\mathrm{kg\,kg^{-1}\,s^{-1}}$); it increases linearly to a value of $-0.174 \times 10^{-5}\,\mathrm{k\,s^{-1}}$ ($-0.19 \times 10^{-8}\,\mathrm{kg\,kg^{-1}\,s^{-1}}$) at 850 hPa, and stays constant above this level.

For the FixHydro case, an ice crystal concentration of $0.16\,\mathrm{L^{-1}}$ (were used as recommended by Klein et al., 2009) and a N_d value of $50\,\mathrm{cm^{-3}}$. For the ObsAero case, the aerosol mass mixing ratios of the three modes were diagnosed from the number mixing ratio and bimodal log-normal size distributions (Eq. 1) with aerosol partitioning of 70 % SO_4 and 30 % primary organic matter (POM) for the accumulation mode and 10 % SO_4, 85 % sea salt, and 5 % dust for the coarse mode. We also used total number concentration, mode radius, and geometric standard deviation of the accumulation ($72.2\,\mathrm{cm^{-3}}$, 0.054 µm, 2.04) and coarse ($1.8\,\mathrm{cm^{-3}}$, 1.3 µm, 2.5) modes, respectively (again following Klein et al., 2009).

c. c.RICO case

Shallow Convection is another important climatological regime. The RICO experiment was conducted on the upwind side of the Islands of Antigua and Barbuda during the winter of 2004 when trade winds cover the northwestern Atlantic Ocean (Rauber et al., 2007). Unlike previous experiments, namely the Atlantic Trade Wind Experiment (ATEX) and Oceanographic and Meteorological Experiment (BOMEX), which did little to measure clouds and precipitation, RICO has extensive cloud-related measurements, which make it an important study for shallow cumulus clouds and precipitation. For this case we tried to set up our case similar to vanZanten et al. (2011). The assumptions made for the RICO case are discussed below.

One unique aspect of the RICO case is that radiation tendencies are included in the prescribed temperature advection tendency. As a result, we had to turn off the shortwave and longwave radiation schemes. There was no nudging applied for this case since specifications were chosen to be energetically and moisture

GMDD
7, 7693–7731, 2014

balanced. Like vanZanten et al. (2011), piecewise linear profiles of u, v, omega, and large-scale forcings of heat and moisture were used. The u value used was $-1.9\,\mathrm{m\,s^{-1}}$ near the surface linearly increasing to $-9.9\,\mathrm{m\,s^{-1}}$ at the top of the boundary layer. The v value was kept constant to $-3.8\,\mathrm{m\,s^{-1}}$. We used a subsidence rate (w_s), which linearly increased from 0 to $-0.5\,\mathrm{cm\,s^{-1}}$ to about 2.2 km and was constant from this level to 4 km, then decreased linearly to zero at the TOA. The large-scale heat forcing was kept constant at a value of $-2.5\,\mathrm{K\,day^{-1}}$, and the moisture forcing profile increased from $-1\,\mathrm{g\,kg^{-1}\,day^{-1}}$ close to the surface to $0.3456\,\mathrm{g\,kg^{-1}\,day^{-1}}$ at about 3 km and was fixed at that value throughout the free troposphere. The driving conditions were created by averaging observations over 16 December 2004 to 8 January 2005.

For the FixHydro case, an observed N_d value of $70\,\mathrm{cm^{-3}}$ was used (vanZanten et al., 2011). For the ObsAero case, the aerosol mass mixing ratios of the three modes were diagnosed from the number mixing ratio and two log-normal size distributions (Eq. 1) assumed to consist of SO_4 with dry density of $1.77\,\mathrm{g\,cm^{-3}}$. We also used a total number, mode radius, and geometric standard deviation $90\,\mathrm{cm^{-3}}$, 0.03 µm, and 1.28 for the aitken mode; $150\,\mathrm{cm^{-3}}$, 0.14 µm, and 1.75 for the accumulation mode. Coarse aerosol mass is assumed to be zero. This specification is recommended by vanZanten et al. (2011).

d. d.ARM95

The ARM95 included because it is the default case, which has long been included with CAM releases. It is also an example of continental convection, which is an important climate regime. The ARM95 case tests the deep convection scheme and to some extent the mixed-phase cloud processes. The case spans 18 July to 3 August 1995, and we used the full shortwave and longwave radiation. Advective forcing was generated by the State University of New York (SUNY) objective analysis method and the surface fluxes were estimated using Doran et al. (1998) surface analysis technique by the Simple Biosphere (SiB2) model (Ghan et al.,

GMDD
7, 7693–7731, 2014

B. Lebassi-Habtezion and P. Caldwell

2000). For this case we only simulated the Default and PrescAero cases because N_d/N_i, and aerosol concentration are unknown.

All the cases were run at the default time step of 1200 s and 30 vertical grid levels with 20 levels in the free troposphere. We carried out four simulations each for DYCOMSRF02, MPACE-B, and RICO and two simulations for ARM95. Results from each method and each case are discussed in the four sections below.

3 Results and discussion

a. a.DYCOMS RF02

Table 1 shows observed and modeled cloud-related variables averaged during the last two hours of the six hour DYCOMS RF02 simulations. In addition to N_d, and surface precipitation (Pr), we include the liquid water path both before and after microphysics was called (LWP_{pre} and LWP_{post}, respectively). These values are different because CAM5 sequentially updates the model state after each parameterization is applied. As described in Gettelman et al. (2014), LWP_{pre} is often much bigger than LWP_{post} because sequential updating leaves microphysical depletion acting over an inappropriately long time step. We also include cloud base z_b computed by interpolating the level where cloud fraction first rises about 0.5 and cloud top height z_i computed by interpolation the highest level where the total water mixing ratio drops below 8 g kg^{-1}. Cloud top entrainment velocity $w_e = \delta z_i/\delta t - w_s$ was also computed.

The Default case underestimated the observed N_d (which was 55 cm^{-3}), while ObsAero and particularly PrescAero overestimated N_d. As expected, runs with higher N_d tend to precipitate less and as a result have higher LWP. LWP computed before microphysics is too high except for the Default case. Values after microphysics show more variability, with the Default case being too low and the FixHydro and PrescAero being too high. Difference between pre- and post-microphysics

GMDD
7, 7693–7731, 2014

values illustrate the difficulty of interpreting output from sequentially-split climate models.

Cloud base and cloud top were both slightly higher than observed yet entrainment was much smaller than observed. This suggests that the subsidence we imposed may be too weak. Surface precipitation is too weak when realistic N_d is used. This could be due to excessive re-evaporation of precipitation below the cloud base. This is consistent with the fact that the ObsAero and FixHydro models have the highest below-cloud base evaporation of precipitation given by 5.85×10^{-8} and $4.45\,kg\,kg^{-1}\,s^{-1}$ respectively, while the Default and PrescAero have lower values (3.62×10^{-8}, and $1.33 \times 10^{-8}\,kg\,kg^{-1}\,s^{-1}$, respectively).

Figure 1a shows N_d profiles of the different aerosol specification cases averaged over the last two hours of the simulation period. We have also included the 10 year July average N_d profile of the corresponding 3-D CAM5 run in which N_d values were extracted at the closest grid point to the DYCOMSRF02 location. All SCM cases showed higher N_d values at the cloud base and slightly lower values at the cloud top. This is inconsistent with observations, which tend to show constant values throughout the cloud (e.g. Martin et al., 1994). The Default model showed the lowest N_d values (an average of $33\,cm^{-3}$). This is probably due to the zero aerosol initialization; aerosol in the run increased as the simulation progressed due to emission sources. The PrescAero case showed highest N_d values (an average of $139\,cm^{-3}$) and the highest total aerosol burden, while the obseAero case showed slightly higher N_d values (an average of $74\,cm^{-3}$) as compared to the observations (an average of $55\,cm^{-3}$), even though it had lower aerosol burden. The 3-D model N_d values are as high as the PrescAero case; however, there is a shift of the whole profile towards the surface, suggesting a collapsed boundary layer.

Even though stratocumulus are non-convective clouds, shallow convection is triggered occasionally, with higher frequency in the Default case than the other cases.

GMDD
7, 7693–7731, 2014

Aerosol specification in single-column CAM5

B. Lebassi-Habtezion and P. Caldwell

Detrainment from this convection is a major source of N_d in some simulations. This occurs because CAM5 detrains droplet numbers according to a fixed droplet mean volume radius assumption rather than considering the actual droplet or aerosol availability. As a result, the convective detrainment from cloud top increased the in-cloud N_d values. In order to separate the number of droplets generated by activation and convective detrainment we conducted another set of sensitivity experiments where vapor rather than condensate is detrained from convection. N_d profiles from these experiments are shown in Fig. 1b. This figure reveals that almost all the droplets in the Default case are created by convective detrainment due to zero aerosol initialization. In the PrescAero and ObsAero cases activation dominates, though detrainment increases the total N_d in all cases, especially near the cloud top.

N_d of DYCOMSRF02 case correlates well with the total aerosol burden. The PrescAero case has the highest aerosol burden resulting in high values of N_d, while the zero-aerosol initialized Default case has the lowest. The ObsAero case has higher aerosol burden in the accumulation and aitken modes resulting in N_d values slightly higher than observed.

Figure 2 shows the temporal evolution of the LWP_{pre} and LWP_{post} of the DYCOMSRF02 case. There is high variability of LWP during the first few hours in all cases, with the highest variability in the Default case. During the last two hours this case performed worst and showed low LWP due to low N_d that caused clouds to precipitate out. The FixHydro and ObsAero cases showed good agreement as compared to the observational ranges. The PrescAero case had higher LWP due to higher N_d values.

In summary, the DYCOMSRF02 case shows strong sensitivity to aerosol specification. In the Default case, detrainment from shallow convection is a major source of N_d, which limits sensitivity to aerosol burden. In other cases, higher aerosol burden translates to higher droplet concentration.

GMDD
7, 7693–7731, 2014

B. Lebassi-Habtezion and P. Caldwell

b. b.MPACE-B

Table 2 shows the observed and modeled cloud-related variables averaged during the last four hours of the MPACE-B case. The variables are N_i, N_d, LWP, IWP, w_e, z_b, z_i, and surf Pr. The N_i values for the Default, PrescAero, and ObsAero cases are 0.4, 0.7, and 0.6 L^{-1}, respectively. All of these cases overestimated the observed N_i value (0.16 L^{-1}). Aircraft and ground based remote sensors observed the existence of boundary layer mixed-phase clouds, which contained liquid and ice and were capped by a weak inversion with a cloud top temperature of about −15 °C (Klein et al., 2009). However, except for the FixHydro case all simulations produced not liquid. This is because ice removes all supersaturated vapor (and liquid) when crystal numbers are too high. The FixHydro case showed reasonable LWP (133 g m^{-2}) and w_e (12.37 mm day^{-1}) due to the realistic use of N_d and N_i; however, it underestimated the IWP (0.63 g m^{-2}) and overestimated z_b (1783 m) and surf Pr (0.5 mm day^{-1}).

Figure 3 shows MPACE-B profiles of liquid water content (LWC) and ice water content (IWC) including and excluding snow mass as a function of scaled height, before and after micro-physics. The dark-shaded region, light-shaded region, and black solid line depict the median value, the inner 50 %, and the outer 50 % envelope of the high frequency observed aircraft data respectively, from Klein et al. (2009). Before microphysics, a reasonable amount of liquid water is shown by the FixHydro case, while the other cases showed shallower cloud and smaller amounts of liquid water (Fig. 3a). After the execution of microphysics, except for the FixHydro case, the microphysics physics removed all the liquid water in the other three models, resulting in complete depletion of liquid water. All cases showed good agreement of IWC as compared to aircraft observations (Fig. 3b and c), with some overestimation of IWC by the FixHydro case. The microphysics slightly removed some IWC from the Default case but did not make any change to the three other cases (Fig. 3b and c). However, IWC consistes entirely of snow

GMDD
7, 7693–7731, 2014

Aerosol specification in single-column CAM5

B. Lebassi-Habtezion and P. Caldwell

except for the FixHydro case, which showed some cloud ice before microphysics (Fig. 3d).

Figure 4 shows the N_i profiles of the different cases averaged over the last four hours of the MPACE-B period. We have also included the 10 years October 2004 average N_i profile values of the 20 min timestep, 30 levels, 3-D CAM run, and values extracted at the closest grid point to the MPACE-B location. Except for the FixHydro case all the other cases overestimated N_i. Despite the difference in the aerosol burden, the Default, PrescAero, and ObsAero cases showed no sensitivity to the aerosol specification except for slightly higher N_i values for the ObsAero case. Similarly, except for the FixHydro case, which had N_d value of 50 cm^{-3}, all the other cases showed N_d value of zero due to the complete depletion of liquid water by the microphysics discussed above. However, all the cases simulated cloud fraction well as compared to aircraft and remote sensing observation (Fig. 5). Reasonable cloud fraction yet zero cloud condensate is possible in CAM5 because cloud fraction is computed before microphysics and is unchanged by physical processes, while cloud mass is affected by subsequent processes.

There exist large uncertainties in the representation of the ice nucleation processes in climate models. In CAM, homogeneous and heterogeneous (deposition, condensation freezing, contact freezing, and immersion freezing) ice nucleation processes in the mixed-phase regime ($-40 < T < -3\,^{\circ}C$) are represented as follows.

Deposition/condensation freezing ice nucleation process is represented by the Meyers et al. (1992) empirical formulation, which only depends on temperature and saturation vapor pressure. Similarly, immersion freezing is prescribed using the formulation of Bigg (1953) and contact freezing on dust is represented using the formulation of Young (1974). Detailed literature of ice nucleation formulation and parameterization for cirrus and mixed phase clouds can be found in Gettelman et al. (2012).

GMDD
7, 7693–7731, 2014

In our SCM simulation of MPACEB, N_i did not show any sensitivity to aerosol specification. This is due to the dominance of the Meyers et al. (1992) deposition/condensation freezing ice nucleation, which does not use explicit aerosol information but only depends on an empirical formulation using temperature and saturation vapor pressure. The other ice nucleation processes did not produce any N_i. The Meyers deposition/condensational freezing depleted all the liquid to form overestimated N_i regardless of the aerosol specification. As a result, activation did not produce any liquid droplets due to the total liquid water depletion.

c. c.RICO

Table 3 shows the averages of N_d, SHF, LHF, Cloud Base Mass Flux (CBMF), Cloud Cover (CLC), and LWP during the last four hours of the 24 h simulation of the RICO case for the four model simulations and from vanZanten et al. (2011) LES results. We use LES as a proxy for truth here because this case is idealized and thus not comparable to observations from any particular time. All the model runs from this study showed similar N_d, SHF, LHF, CBMF, CLC, and LWP values when compared to one another. The Default, PrescAero, and ObsAero cases showed an average N_d value of 51 cm^{-3}, which slightly underestimated the LES value (70 cm^{-3}), which is a best estimate of an average value from flight measurements using the Fast Forward Scattering Spectrometer Probe (FFSSP) during four flights, with measurements ranging from 50 to 100 cm^{-3} (vanZanten el al., 2011; Brenguir et al., 1998). On average all the runs overestimated the LHF (12.7 $W m^{-2}$), LHF (207.9 $W m^{-2}$), and CBMF (0.06 $m s^{-1}$) as compared to the LES value (8.5 $W m^{-2}$, 158 $W m^{-2}$, 0.026 $m s^{-1}$), respectively. All the models simulated CLC (0.18), and LWP (19.4 $g m^{-2}$) very well as compared to LES, (0.19) and (19 $g m^{-2}$), respectively. The time series of the LWP shown in Fig. 6 also depicts high variability during the spin-up period and good agreement with LES after 15:00 UTC for all models.

GMDD
7, 7693–7731, 2014

Figure 7 shows the N_d profiles of all the cases of this study averaged over the last 4 h of the simulation period. We have also included the 10 years July average N_d profile values of the 20 min timestep and 30 levels 3-D CAM extracted at the closest grid point to the RICO location. The PrescAero, the Default and 3-D has similar values of N_d at the cloud base where the statiform cloud was present. However, the N_d value is underestimated as compared to observations (70 cm^{-3}). The ObsAero case showed the lowest N_d (about 14 cm^{-3}). At the cloud top, except for the FixHydro case, all the SCM cases showed N_d values approaching the no aerosol case (black line). The no aerosol case was run without aerosols to estimate the N_d values due to convective detrainment.

The N_d of the RICO case at the cloud base correlates well with the different aerosol burden values in the different modes. The PrescAero and Default cases have comparable N_d values due to high aerosol burden. The ObsAero case shows the lowest N_d values at the cloud base due to its low aerosol burden. Hence, the activation process is dominant at the cloud base in creating the droplets. However, at the cloud top, despite the differences in the aerosol specifications, the N_d values did not change. Thus activation is the dominant process at the cloud base while detrainment dominates at the cloud top.

Vertical structure of the cloud mass flux and condensate is important for studying the parameterization of clouds and precipitation. Shallow convective mass flux maximizes near the cloud base and decreases with height, consistent with observations (Siebesma et al., 2003). However, the mass flux at the cloud base is overestimated in all the cases (Fig. 8a). Unsurprisingly, the condensate profile also shows overpredicted condensate at the cloud base and decreases with height (Fig. 8b).

The total cloud fraction is also overestimated as compared to LES (Fig. 9). At cloud base the overestimation due to both shallow convective and stratiform clouds. Modeled cloud extends further into the troposphere than observed

GMDD
7, 7693–7731, 2014

because deep convection is being triggered and the runs showed deeper clouds due to the deep convective cloud fraction (Fig. 9). Non of the runs show sensitivity of mass flux, condensate, and cloud fraction to aerosol specification.

In summary, the RICO runs did not show sensitivity to aerosol specification except at the cloud base where activation dominates and more droplets are formed as the aerosol burden increases. At the cloud top, detrainment is dominant and regardless of the aerosol burden the N_d profiles are similar.

d. d.ARM95

The last case is based on ARM SGP site and spans 17 days starting 18 July to 4 August 1995. It was chosen because it is the default SCM case distributed with CAM5. This case is the basis of the Ghan et al. (2000) SCM intercomparison. Only the Default and the PrescAero cases are simulated due to lack of observed N_d, N_i and aerosol data.

This case spans 3 different weather regimes. Due to the existence of a large-scale stationary upper-level trough over the continental US during the first ten-day period, there existed variable cloud cover and precipitation every other day. There followed a 3 day period of high pressure and clear skies, and the final 7 days consisted of stormy weather with high cloud cover and intense precipitation.

Figure 10 shows the time series of LWP and IWP for the Default and PrescAero cases. The time series of the LWP observations are also plotted from Xu and Randall (2000). Generally, SCAM over estimated LWP at all periods. Both runs showed comparable LWP, IWP, and surface precipitation (Fig. 10) as well as N_d (Fig. 11). Aerosol optical depth in the visible range was 0.163 for PrescAero and only 0.081 for the Default case, however, indicating that the ARM95 case is insensitive to aerosol specification. As noted above, this result is not surprising since CAM's convective schemes do not use aerosol information. More surprising, however, is the fact that N_d for the SGP region from both SCM and GCM simulations is $\sim 25\,\text{cm}^{-3}$, a factor of 8 smaller than typically observed in this region (e.g.

GMDD
7, 7693–7731, 2014

Iacobellis and Somerville, 2006). This is a major bias in cloud properties which likely has significant negative effects on climate simulations.

4 Summary and conclusions

In this study we identified a problem with SCAM5 in its default configuration and introduced fixes to the identified problem. We used three new aerosol specification methods in our SCM simulations. The aerosol cases considered are Default case (with prognostic aerosol, initialized to zero), PrescAero case (with monthly climatological aerosol values), ObsAerosol case (with aerosols from observations), and the FixHydro case (with fixed droplet and ice crystal concentrations). We use SCM simulations for a variety of cloud regimes. The sites used for these studies include summertime mid-latitude continental convection (ARM95), shallow convection (RICO), subtropical drizzling stratocumulus (DYCOMSRF02), and multi-level Arctic clouds (MPACE-B).

The DYCOMSRF02 case shows strong sensitivity to aerosol specification. Activation dominates over convective detrainment so a number of droplets are formed when you have higher aerosol burden. Convection does occur in all runs, however, and convective detrainment is source of N_d in all cases, regardless of the aerosol specification. Default aerosol treatment in DYCOMSRF02 produced greatly underestimated N_d and LWP. All proposed fixes substantially improve N_d and LWP.

In MPACE-B, N_i was too large and was insensitive to aerosol specification in all cases except FixHydro. This is due to the dominance of the Meyers et al. (1992) deposition/condensation freezing ice nucleation, which does not use aerosol information but only depends on empirical formulation using temperature and saturation vapor pressure. The other ice nucleation processes did not produce any N_i. The Meyers deposition/condensational freezing was also too strong, causing all supersaturated vapor to freeze. This resulted in zero LWP for all cases except FixHydro, which had LWP value of 30 g m^{-2} (in agreement with observations).

GMDD
7, 7693–7731, 2014

Aerosol specification in single-column CAM5

B. Lebassi-Habtezion and P. Caldwell

The RICO case did not show sensitivity to aerosol specification except at the cloud base where activation dominates and more droplets are formed as the aerosol burden increases. At the cloud top, convective detrainment is the dominant source of droplets, and regardless of the aerosol burden the number of droplets is similar. Detrainment seems to be too strong near cloud base, resulting in profile with too much cloud near cloud base and too little above.

The deep-convection ARM95 case also did not show any sensitivity to aerosol specification. Droplet number for both SCM and GCM runs at ARM95 were consistently 25 cm^{-3}, which is much lower than expected over land. This indicates a problem with aerosol specification in this region.

In summary, stratiform cloud cases (DYCOMS RF02 and MPACE-B) were found to have a strong dependence on aerosol concentration, while convective cases (RICO and ARM95) were relatively insensitive to aerosol specification. This is perhaps expected because convective schemes in CAM5 do not currently use aerosol information. Adequate liquid water content in the MPACE-B case was only maintained when ice crystal number concentration was specified because the Meyers et al. (1992) deposition/condensation ice nucleation scheme used by CAM5 greatly overpredicts ice nucleation rates, causing clouds to rapidly glaciate. Surprisingly, predicted droplet concentrations for the ARM95 region in both SCM and global runs were around 25 cm^{-3}, which is much lower than observed. This finding suggests that CAM5 has problems capturing aerosol effects in this region.

Acknowledgements. We thank the Lawrence Livermore National Laboratory (LLNL) for providing funding through the Scientific Discovery through Advanced Computing (SciDAC) project. The SCM simulations were performed using computing resources provided by LLNL. The research reported here was supported by DOE award 33871/SCW1316-BER and was performed under the auspices of the United States Department of Energy by Lawrence Livermore National Laboratory under contract DE-AC52-07NA27344.

References

Abdul-Razzak, H. and Ghan, S.: A parameterization of aerosol activation: 2. Multiple aerosol types, J. Geophys. Res., 105, 6837–6844, 2000.

Ackerman, A. S., vanZanten, M. C., Stevens, B., Savic-Jovcic, V., Bretherton, C. S., Chlond, A., Golax, J-C., Jiang, H., Khairoutdinov, M., Krueger, S. K., Lewellen, D. C., Lock, A., Moeng, C-H., Nakamura, K., Petters, D. M., Snider, J. R., Weinbrecht, S., and Zulauf, M.: Large-eddy simulations of a drizzling, stratocumulus-topped marine boundary layer, Mon. Weather Rev., 137, 1083–1110, doi:10.1175/2008MWR2582.1, 2009.

Bigg, E. K.: The formation of atmospheric ice crystals by the freezing of droplets, Q. J. Roy. Meteor. Soc., 79, 510–519, 1953.

Bony, S. and Dufresne, J.-L.: Marine boundary layer clouds at the heart of tropical cloud feedback uncertainties in climate models, Geophys. Res. Lett., 32, L20806, doi:10.1029/2005GL023851, 2005.

Brenguier, J. L., Bourrianne, T., de Araujo Coelho, A., Isbert, R. J., Peytavi, R., Trevarin, D., and Weschler, P.: Improvements of droplet distribution size measurements with the fast-FSSP (forward scattering spectrometer probe), J. Atmos. Ocean. Tech., 15, 1077–1090, 1998.

Bretherton, C. S. and Park, S.: A new moist turbulence parameterization in the community atmosphere model, J. Climate, 22, 3422–3448, 2009.

Doran, J. C., Hubbe, J. M., Liljegren, J. C., Shaw, W. J., Collatz, G. J., Cook, D. R., and Hart, R. L.: A technique for determining the spatial and temporal distributions of surface fluxes of heat and moisture over the Southern Great Plains Cloud and Radiation Testbed, J. Geophys. Res., 103, 6109–6121, doi:10.1029/97JD03427, 1998.

Easter, R. C., Ghan, S. J., Zhang, Y., Saylor, R. D., Chapman, E. G., Laulainen, N. S., Abdul-Razzak, H., Leung, L. R., Bian, X., and Zaveri, R. A.: MIRAGE: model description and evaluation of aerosols and trace gases, J. Geophys. Res., 109, D20210, doi:10.1029/2004JD004571, 2004.

Forster, P., Ramaswamy, V., Artaxo, P., Berntsen, T., Betts, R., Fahey, D. W., Haywood, J., Lean, J., Lowe, D. C., Myhre, G., Nganga, J., Prinn, R., Raga, G., Schulz, M., and Dorland, R. V.: Changes in atmospheric constituents and in radiative forcing, in: Climate Change: The Physical Science Basis, Contribution of Working Group I to the Fourth Assessment Report of the Intergovernmental Panel on Climate Change, edited by: Solomon, S., Qin, D., Manning, M., Chen, Z., Marquis, M., Averyt, K. B., Tignor, M., and Miller, H. L., Cambridge Univ. Press, UK and New York, 2007.

Gettelman, A., Morrison, H., and Ghan, S. J.: A new two-moment bulk stratiform cloud microphysics scheme in the NCAR Community Atmosphere Model (CAM3), Part II: Single-column and global results, J. Climate, 21, 3660–3679, 2008.

Gettelman, A., Liu, X., Barahona, D., Lohmann, U., and Chen, C.: Climate impacts of ice nucleation, J. Geophys. Res., 117, D20201, doi:10.1029/2012JD017950, 2012.

Gettelman, A., Morrison, H., Santos, S., Bogenschutz, P., and Caldwell, P. H.: Advanced two-moment microphysics for global models. Part II: Global model solutions and aerosol-cloud interactions, J. Climate, doi:10.1175/JCLI-D-14-00103.1, in press, 2014.

Ghan, S. J., Randall, D., Xu, K-M., Cederwall, R., Cripe, D., Hack, J., Iacobellis, S., Klein, S., Krueger, S., Lohmann, U., Pedretti, J., Robock, A., Rotstayn, L., Somerville, R., Stenchikov, G., Sud, Y., Walker, G., Xie, S., Yio, J., Zhang, M.: A comparison of single column model simulations of summertime midlatitude continental convection, J. Geophys. Res., 105, 2091–2124, 2000.

Ghan, S. J., Liu, X., Easter, R. C., Zaveri, R., Rasch, P. J., Yoon, J.-H., and Eaton, B.: Toward a minimal representation of aerosols in climate models: comparative decomposition of aerosol direct, semidirect, and indirect radiative forcing, J. Climate, 25, 6461–6476, doi:10.1175/JCLI-D-11-00650.1, 2012.

Hack, J. J. and Pedretti, J. A.: Assessment of solution uncertainties in single-column modeling frameworks, J. Climate, 13, 352–365, doi:10.1175/1520-0442(2000)013<0352:AOSUIS>2.0.CO;2, 2000.

Hartmann, D. L., Ockert-Bell, M. E., and Michelsen, M. L.: The effect of cloud type on earth's energy balance: global analysis, J. Climate, 5, 1281–1304, 1992.

Haywood, J. M. and Boucher, O.: Estimates of the direct and indirect radiative forcing due to tropospheric aerosols, 2000: a review, Rev. Geophys., 38, 51–543, doi:10.1029/1999RG000078, 2000.

Houghton, J. T., Filho, L. G. M., Callander, B. A., Harris, N., Kattenberg, A., and Maskell, K. (Eds.): Intergovernmental Panel on Climate Change, Climate Change: The Science of Climate Change, The Contribution of Working Group I to the Second Assessment Report of the IPCC, Cambridge Univ. Press, New York, 1995.

GMDD
7, 7693–7731, 2014
Aerosol specification in single-column CAM5
B. Lebassi-Habtezion and P. Caldwell

Iacobellis, S. F. and Somerville, R. C. J.: Evaluating parameterizations of the autoconversion process using a single-column model and Atmospheric Radiation Measurement Program measurements, J. Geophys. Res., 111, D02203, doi:10.1029/2005JD006296, 2006.

Klein, S. A., McCoy, R. B., Morrison, H., Ackerman, A. S., Avramov, A., de Boer, G., Chen, M., Cole, J. N. S., Del Genio, A. D., Falk, M., Foster, M. J., Fridlind, A., Golaz, J.-C., Hashino, T., Harrington, J. Y., Hoose, C., Khairoutdinov, M. F., Larson, V. E., Liu, X., Luo, Y., McFarquhar, G. Y., Menon, S., Neggers, R. A. J., Park, S., Poellot, M. R., Schmidt, J. M., Sednev, I., Shipway, B. J., Shupe, M. D., Spangenberg, D. A., Sud, Y. C., Turner, D. D., Veron, D. E., von Salzen, K., Walker, G. K., Wang, Z., Wolf, A. B., Xie, S., Xu, K-M., Yang, F., and Zhang, G.: Intercomparison of model simulations of mixed-phase clouds observed during the ARM Mixed-Phase Arctic Cloud Experiment. Part I: Single-layer cloud., Q. J. Roy. Meteor. Soc., 135, 979–1002, doi:10.1002/qj.416, 2009.

Liu, X., Easter, R. C., Ghan, S. J., Zaveri, R., Rasch, P., Shi, X., Lamarque, J.-F., Gettelman, A., Morrison, H., Vitt, F., Conley, A., Park, S., Neale, R., Hannay, C., Ekman, A. M. L., Hess, P., Mahowald, N., Collins, W., Iacono, M. J., Bretherton, C. S., Flanner, M. G., and Mitchell, D.: Toward a minimal representation of aerosols in climate models: description and evaluation in the Community Atmosphere Model CAM5, Geosci. Model Dev., 5, 709–739, doi:10.5194/gmd-5-709-2012, 2012.

Martin, G. M., Johnson, D. W., and Spice, A.: The measurement and parameterization of effective radius of droplets in warm stratocumulus clouds, J. Atmos. Sci., 51, 1823–1842, 1994.

Meyers, M. P., DeMott, P. J., and Cotton, W. R.: New primary ice-nucleation parameterizations in an explicit cloud model, J. Appl. Meteorol., 3, 708–721, 1992.

Mlawer, E. J., Taubman, S. J., Brown, P. D., Iacono, M. J., and Clough, S. A.: Radiative transfer for inhomogeneous atmosphere: RRTM, a validated correlated-k model for the longwave, J. Geophys. Res., 102, 16663–16682, 1997.

Moeng, C., H., Cotton, W. R., Bretherton, C. S., Chlond, A., Khairoutdinov, M., Krueger, S., Lewellen, W. S., MacVean, M. K., Pasquier, J. R. M., Rand, H. A., Siebesma, A. P., Sykes, R. I., and Stevens, B.: Simulation of a stratocumulus-topped PBL: intercomparison among different numerical codes, B. Am. Meteorol. Soc., 77, 261–27, 1996.

Morrison H. and Gettelman, A.: A new two-moment bulk stratiform cloud microphysics scheme in the Community Atmosphere Model, version 3 (CAM3). Part I: Description and numerical tests, J. Climate, 21, 3642–3659, 2008.

GMDD
7, 7693–7731, 2014

Aerosol specification in single-column CAM5

B. Lebassi-Habtezion and P. Caldwell

Park, S. and Bretherton, C. S.: The University of Washington shallow convection and moist turbulence schemes and their impact on climate simulations with the community atmosphere model, J. Climate, 22, 3449–3469, doi:10.1175/2008JCLI2557.1, 2009.

Park, S., Bretherton, C. S., and Rasch, P. J.: Integrating cloud processes in the community atmosphere model, version 5, J. Climate, 27, 6821–6856, doi:10.1175/JCLI-D-14-00087.1, 2014.

Rauber, R. M., Ochs III, H. T., Di Girolamo, L., Göke, S., Snodgrass, E., Stevens, B., Knight, C., Jensen, J. B., Lenschow, D. H., Rilling, R. A., Rogers, D. C., Stith, J. L., Albrecht, B. A., Zuidema, P., Blyth, A. M., Fairall, C. W., Brewer, W. A., Tucker, S., Lasher-Trapp, S. G., Mayol-Bracero, O. L., Vali, G., Geerts, B., Anderson, J. R., Baker, B. A., Lawson, R. P., Bandy, A. R., Thornton, D. C., Burnet, E., Brenguier, J.-L., Gomes, L., Brown, P. R. A., Chuang, P., Cotton, W. R., Gerber, H., Heikes, B. G., Hudson, J. G., Kollias, P., Krueger, S. K., Nuijens, L., O'Sullivan, D. W., Siebesma, A. P., and Twohy, C. H.: Rain in shallow cumulus over the ocean: the RICO campaign, B. Am. Meteorol. Soc., 88, 1912–1928, 2007.

Siebesma, A. P., Bretherton, C. S., Brown, A., Chlond, A., Cuxart, J., Duynkerke, P. J., Jiang, H., Khairoutdinov, M., Lewellen, D., Moeng, C-H., Sanchez, E., Stevens, B., and Stevens, D. E.: A large eddy simulation intercomparison study of shallow cumulus convection, J. Atmos. Sci., 60, 1201–1219, 2003.

Stevens, B., Moeng, C.-H., Ackerman, A. S., Bretherton, C. S., Chlond, A., de Roode, S., Edwards, J., Golaz, J.-C., Jiang, H., Khairoutdinov, M., Kirkpatrick, M. P., Lewellen, D. C., Lock, A., Muller, F., Stevens, D. E., Whelan, E., and Zhu, P.: Evaluation of large-eddy simulations via observations of nocturnal marine stratocumulus, Mon. Weather Rev., 133, 1443–1462, 2005.

vanZanten, M. C. and Stevens, B.: Observations of the structure of heavily precipitating marine stratocumulus, J. Atmos. Sci., 62, 4327–4342, doi:10.1175/JAS3611.1, 2005.

vanZanten, M. C., Stevens, B., Nuijens, L., Siebesma, A. P., Ackerman, A. S., Burnet, F., Cheng, A., Couvreux, F., Jiang, H., Khairoutdinov, M., Kogan, Y., Lewellen, D. C., Mechem, D., Nakamura, K., Noda, A., Shipway, B. J., Slawinska, J., Wang, S., and Wyszogrodzki, A.: : Controls on precipitation and cloudiness in simulations of trade-wind cumulus as observed during RICO, J. Adv. Model. Earth Syst., 3, M06001, doi:10.1029/2011MS000056, 2011.

Wyant, M. C., Bretherton, C. S., Chlond, A., Griffin, B. M., Kitagawa, H., Lappen, C. L., Larson, V. E., Lock, A., Park, S., de Roode, S. R., Zhao M., and Ackerman, A. S.: A single-column

model intercomparison of a heavily drizzling stratocumulus-topped boundary layer, J. Geophys. Res., 112, D24204, doi:10.1029/2007JD008536, 2007.
Xu, K.-M. and Randall, D. A.: Explicit simulation of midlatitude cumulus ensembles: comparison with ARM data, J. Atmos. Sci., 57, 2839–2858, doi:10.1175/1520-0469(2000)057<2839:ESOMCE>2.0.CO;2, 2000.
Young, K. C.: The role of contact nucleation in ice phase initiation of clouds, J. Atmos. Sci., 31, 768–776, 1974.
Zhang, G. J. and McFarlane, N. A.: Sensitivity of climate simulate simulation to the parameterization of cumulus convection in the Canadian Climate center general circulation model, Atmos. Ocean, 33, 407–446, 1995.
Zhu, P., Bretherton, C. S., Köhler, M., Cheng, A., Chlond, A., Geng, Q., Austin, P., Golaz, J.-C., Lenderink, G., Lock, A., and Stevens, B.: Intercomparison and interpretation of single-column model simulations of a nocturnal stratocumulus-topped marine boundary layer, Mon. Weather Rev., 133, 2741–2758, doi:10.1175/MWR2997.1, 2005.

GMDD
7, 7693–7731, 2014

Aerosol specification in single-column CAM5

B. Lebassi-Habtezion and P. Caldwell

Table 1. Averages of N_d, N_i, w_e, z_b, z_i, and Surf Pr during the last two hours of the 6 h DY-COMSRF02 simulations. The observations are from Wyant et al. (2007).

	N_d (cm^{-3}), N_i (L^{-1})	LWP_{pre} ($g\,m^{-2}$)	LWP_{post} ($g\,m^{-2}$)	w_e ($mm\,s^{-1}$)	z_b (m)	z_i (m)	Surf Pr ($mm\,day^{-1}$)
Observation	55, 0	80–120	80–120	6–7.6	~ 450	~ 800	0.35
Default	33, 0	103	73	4.2	475	803	0.31
PrescAero	139, 0	137	126	4.0	473	816	0.04
ObsAero	74, 0	146	119	3.4	492	815	8.5×10^{-6}
FixHydro	55, 0	174	145	3.6	465	818	6.9×10^{-6}

GMDD
7, 7693–7731, 2014

Aerosol specification in single-column CAM5

B. Lebassi-Habtezion and P. Caldwell

GMDD

7, 7693–7731, 2014

Aerosol specification in single-column CAM5

B. Lebassi-Habtezion and P. Caldwell

Table 2. Averages of N_d, N_i, w_e, z_b, z_i, and Surf Pr during the last four hours of the 12 h MPACEB case simulations. The observations are from Klein et al. (2009).

	N_i (L^{-1}), N_d (cm^{-3})	LWP ($g\,m^{-2}$)	IWP ($g\,m^{-2}$)	w_e ($mm\,s^{-1}$)	z_b (m)	z_i (m)	Surf Pr ($mm\,day^{-1}$)
Observation	0.16, 50	110–210	8–30		600	1500	0.25
Default	0.4, 0	3.96×10^{-9}	0.022	11.46	918	1476	0.82
PrescAero	0.7, 0	3.69×10^{-9}	0.018	15.37	984	1537	0.69
ObsAero	0.6, 0	3.64×10^{-9}	0.014	15.37	985	1537	0.68
FixHydro	0.16, 50	133	0.63	12.37	872	1783	0.50

Table 3. Averages of N_d, SHF, LHF, CBMF, Cloud Cover, and LWP during the last four hours of the 24 h simulations at RICO. LES data are from vanZanten et al. (2011).

	N_d(cm^{-3})	SHF ($W m^{-2}$)	LHF ($W m^{-2}$)	CBMF ($m s^{-1}$)	Cloud Cover	LWP ($g m^{-2}$)
LES	70	8.5	158	0.026	0.19	19
Default	30	12.29	207.81	0.06	0.18	19.0
PrescAero	32	12.41	207.94	0.06	0.18	19.2
ObsAero	14	12.42	207.83	0.06	0.18	19.8
FixHydro	70	12.37	207.83	0.06	0.18	19.6

GMDD
7, 7693–7731, 2014

B. Lebassi-Habtezion and P. Caldwell

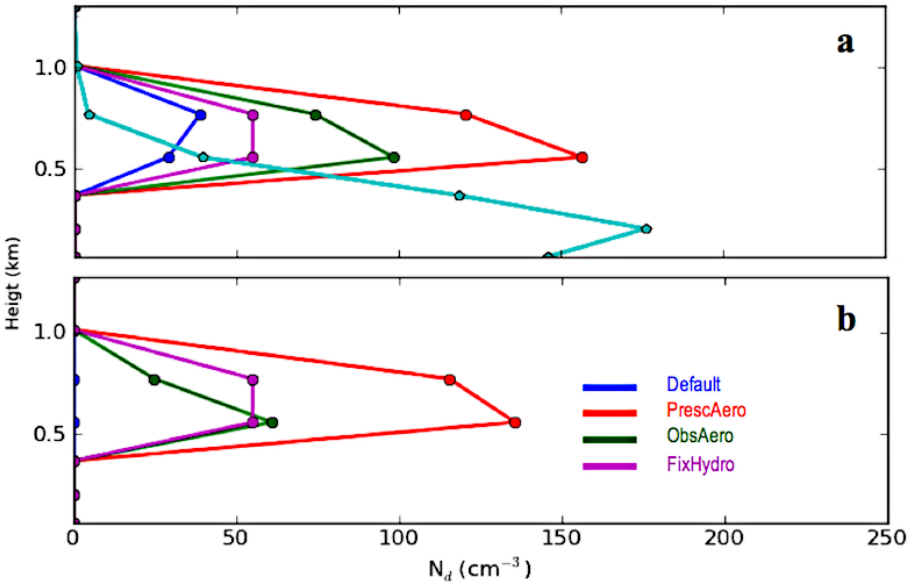

Figure 1. Profiles of in-cloud droplet number concentrations (N_d) for DYCOMSRF02. 3-D CAM values are 10 years July average global CAM extracted at the location of DYCOMSRF02. **(a)** Convective detrainment turned on **(b)** convective detrainment turned off.

GMDD
7, 7693–7731, 2014

Aerosol specification in single-column CAM5

B. Lebassi-Habtezion and P. Caldwell

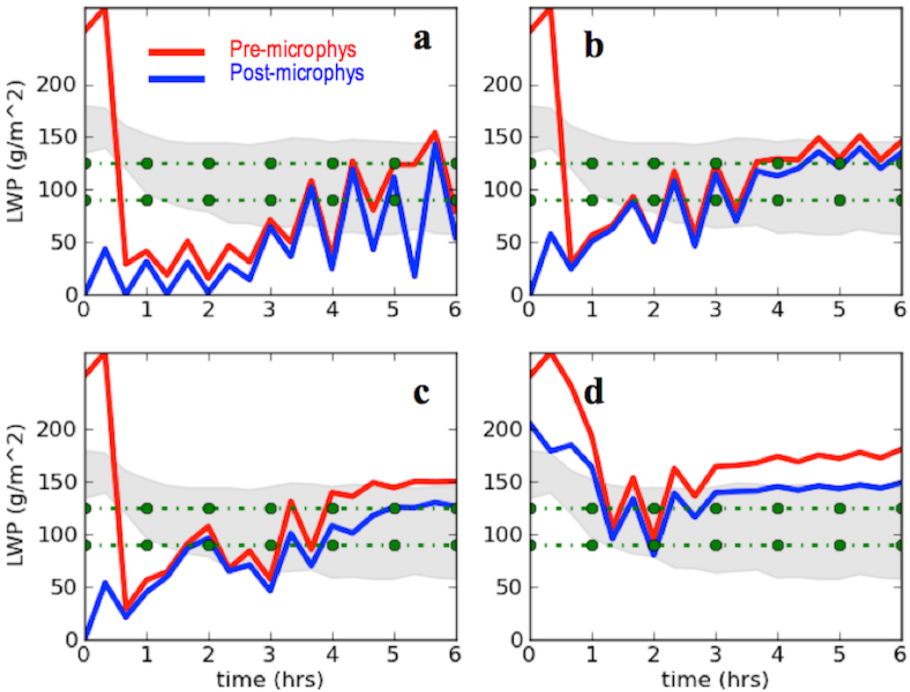

Figure 2. Time series of liquid water path (LWP) for DYCOMSRF02 case for the 6 h simulation period. Red = before microphysics; Blue = after microphysics. The shaded area indicates the range of the LES values averaged over the last 4 h of the simulation period (Stevens and Seifert, 2008). The dots indicate the approximate measurement (what the measurements are) ranges (from Stevens et al., 2003). **(a)** Default case, **(b)** PrescAero case, **(c)** ObsAero case and **(d)** FixHydro case.

GMDD
7, 7693–7731, 2014

Aerosol specification in single-column CAM5

B. Lebassi-Habtezion and P. Caldwell

Title Page
Abstract | Introduction
Conclusions | References
Tables | Figures
◂◂ | ▸▸
◂ | ▸
Back | Close
Full Screen / Esc
Printer-friendly Version
Interactive Discussion

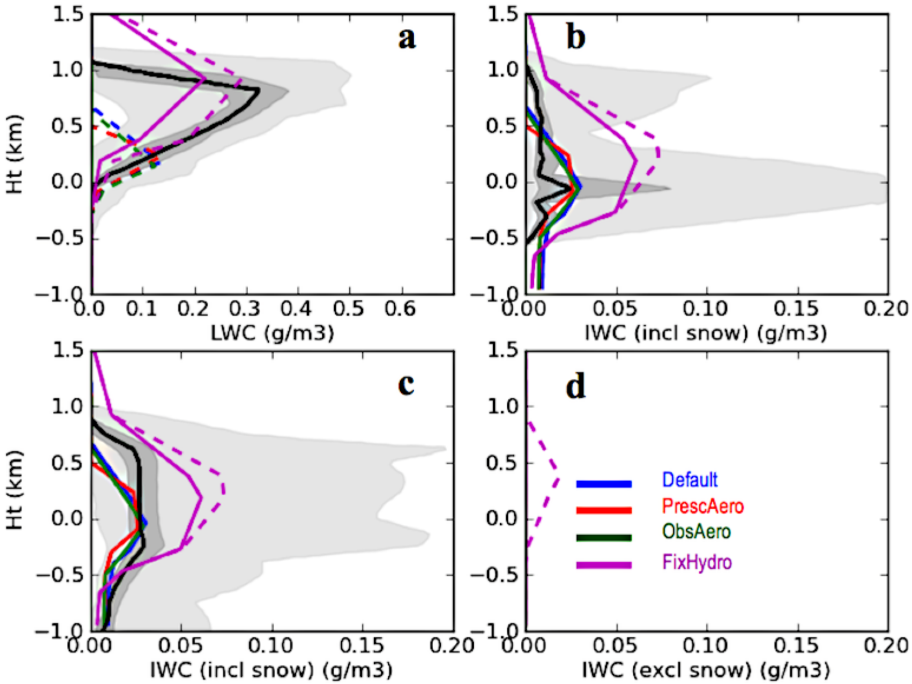

Figure 3. Profiles of liquid water content (LWC) and ice water content (IWC) as function of scaled height ($z/z_b - 1$) for MPACEB. Dashed lines indicate values before microphysics and solid lines indicate values after microphysics. **(a)** LWC profiles as function of scaled height. Dark shaded region ranges, light shaded region and black solid line depict the median value, the inner 50 % and the outer 50 % the envelope of the high frequency observed aircraft data respectively (from Klein et al., 2009). **(b)** The same as Fig. 3a but for IWC (including snow). **(c)** Same as Fig. 6a but using radar data as observations. **(d)** Same as Fig. 3a but excluding snow.

GMDD
7, 7693–7731, 2014

Aerosol specification in single-column CAM5

B. Lebassi-Habtezion and P. Caldwell

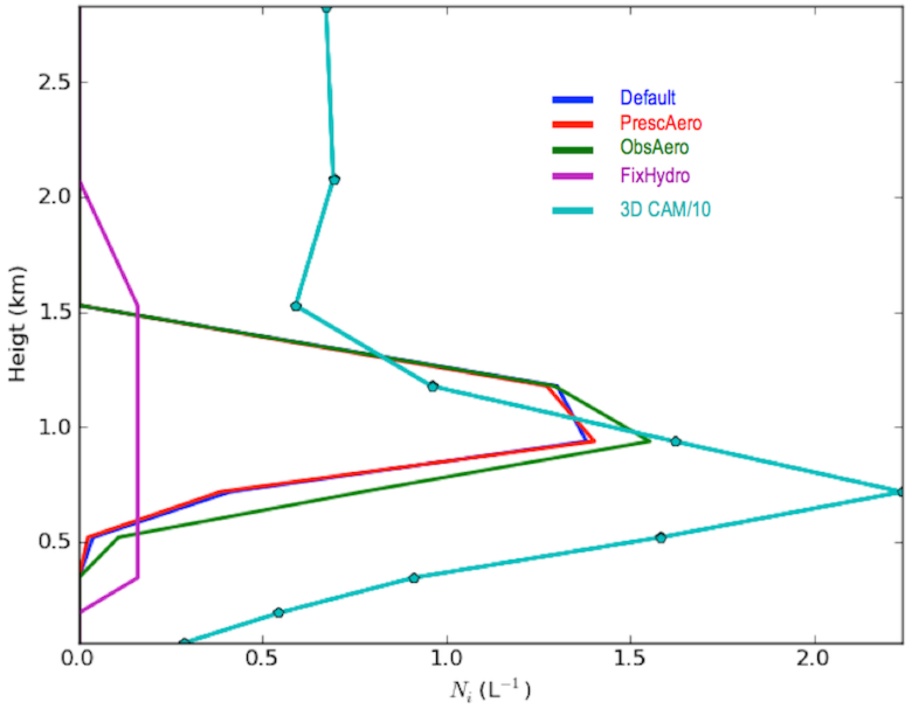

Figure 4. Profiles of in-cloud N_i values for MPACE-B case. 3-D CAM values are 10 years July average global CAM extracted at the location of MPACE-B. Note: N_i values (3-D CAM N_i are divided by 10 to fit in the plot).

GMDD
7, 7693–7731, 2014

Aerosol specification in single-column CAM5

B. Lebassi-Habtezion and P. Caldwell

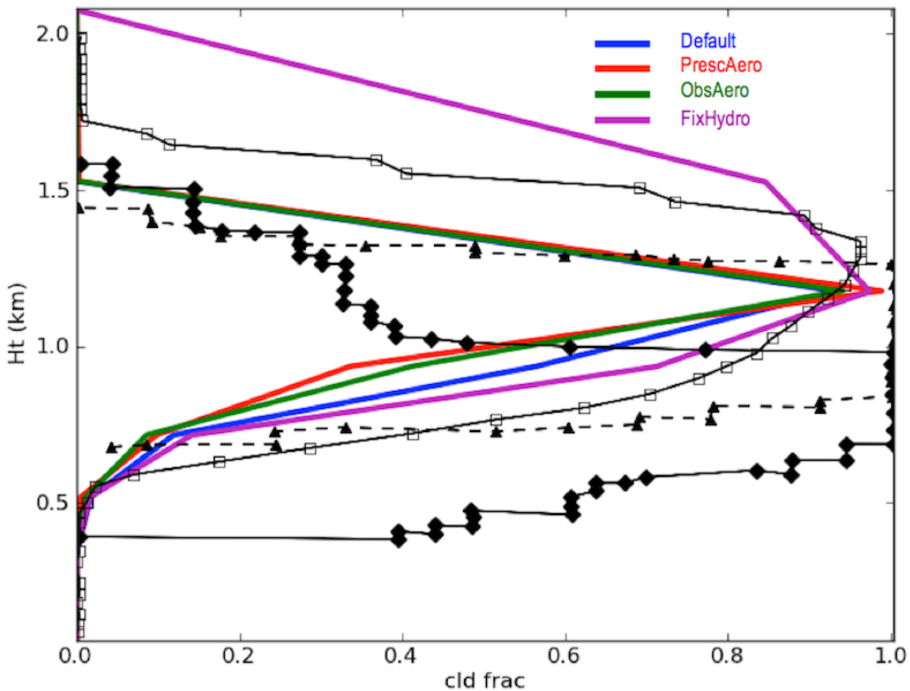

Figure 5. Time-averaged profiles of cloud cover from models and observations as function of height during the MPACE IOP period. The observations panel depicts the fraction of time at each height that cloud was observed from remote sensors (black line with open squares) at Barrow (SHUPE-TURNER) and the two aircraft flights (aircraft 1 dashed line with solid triangle, aircraft 2 solid line with solid diamond). Observations are from Klein et al. (2009).

GMDD
7, 7693–7731, 2014

Aerosol specification in single-column CAM5

B. Lebassi-Habtezion and P. Caldwell

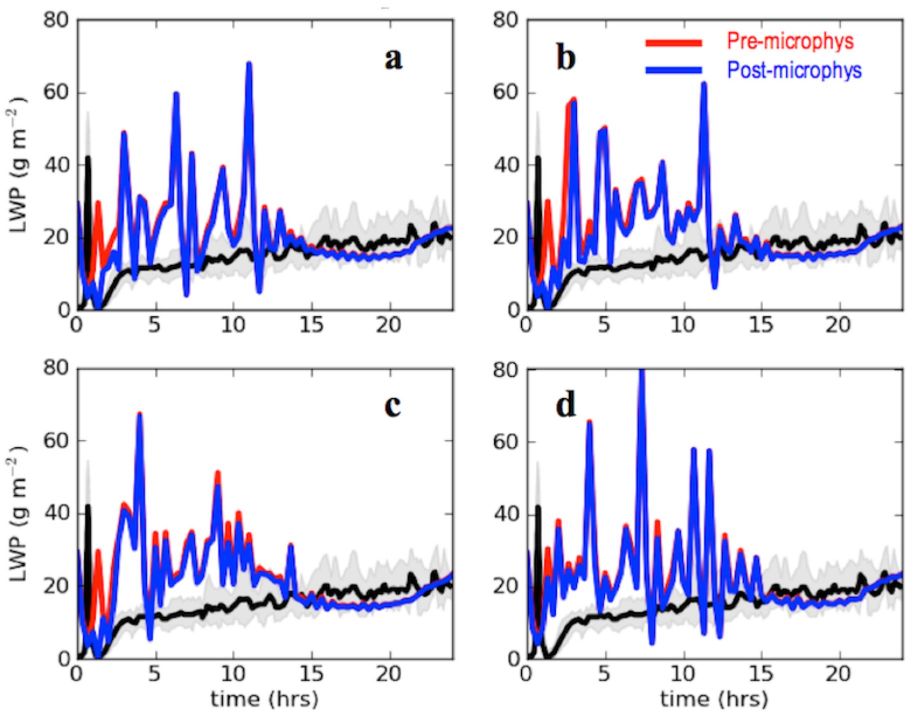

Figure 6. Time series of liquid water path (LWP) during the RICO IOP period. Red = before microphysics and Blue = after microphysics. **(a)** Default case, **(b)** PrescAero case, **(c)** ObsAero case and **(d)** FixHydro case.

GMDD
7, 7693–7731, 2014

B. Lebassi-Habtezion and P. Caldwell

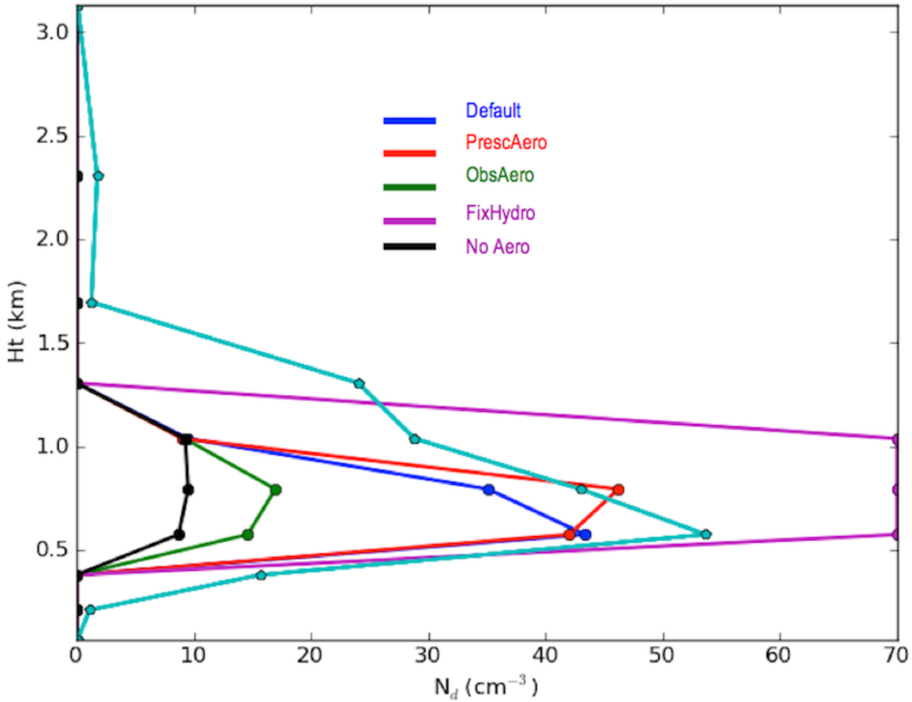

Figure 7. The same as Fig. 1 but for RICO case.

GMDD
7, 7693–7731, 2014

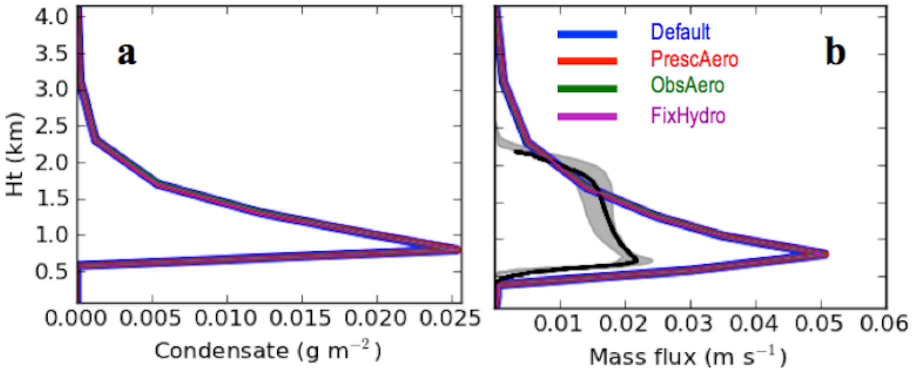

Figure 8. Time-averaged profiles of condensate amount **(a)**, and mass-flux profile **(b)** during RICO IOP. Colors indication the four cases (but are not all visible because the lay on top of one another). Shading in **(b)** indicates ensemble inter quartile range and the solid black line is the ensemble mean. LES data are from vanZanten et al. (2011).

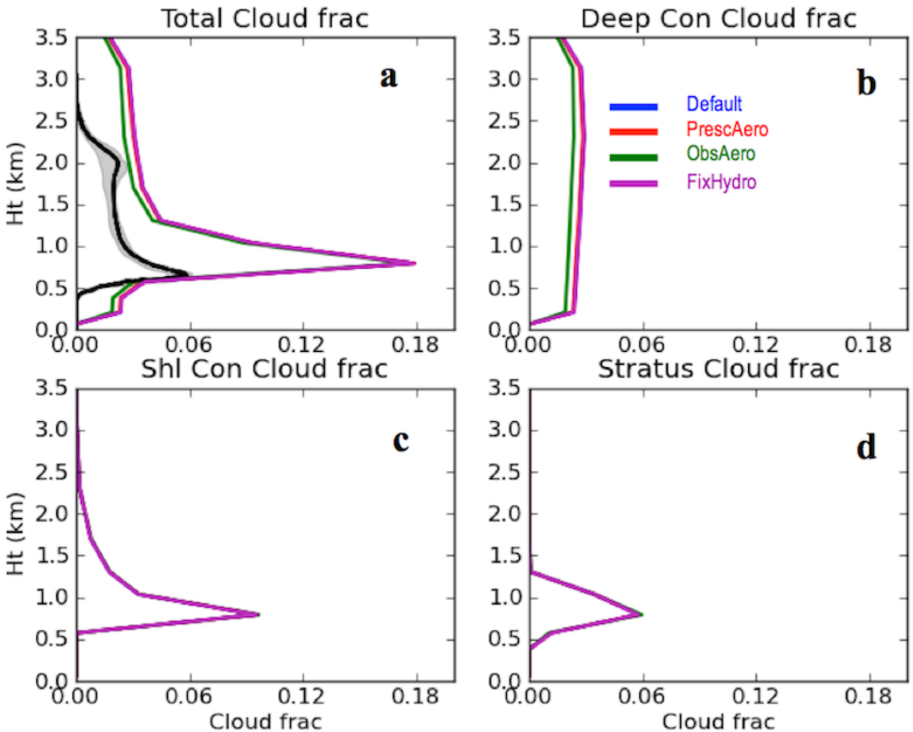

Figure 9. Time-averaged profiles of: **(a)** total cloud cover, **(b)** deep convective cloud fraction, **(c)** shallow convective cloud fraction, and **(d)** stratiform cloud fraction from models and LES as function of height during the RICO IOP period (but are not all visible because the lay on top of one another). Shading indicates total cloud cover ensemble inter quartile range and the solid black line is the ensemble mean. LES data are from vanZanten et al. (2011).

GMDD
7, 7693–7731, 2014

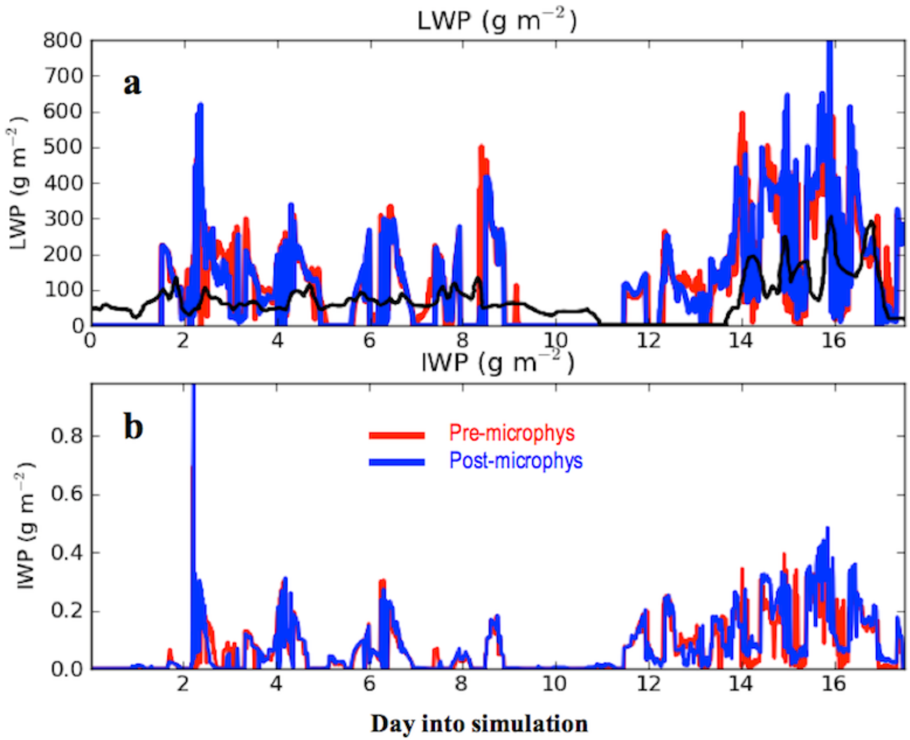

Figure 10. Time series of: **(a)** LWP and **(b)** IWC during the ARM95 IOP period. Red = Default and Blue = PrescAero. The solid black line is observations from Xu and Randall (2000).

GMDD
7, 7693–7731, 2014

Aerosol specification in single-column CAM5

B. Lebassi-Habtezion and P. Caldwell

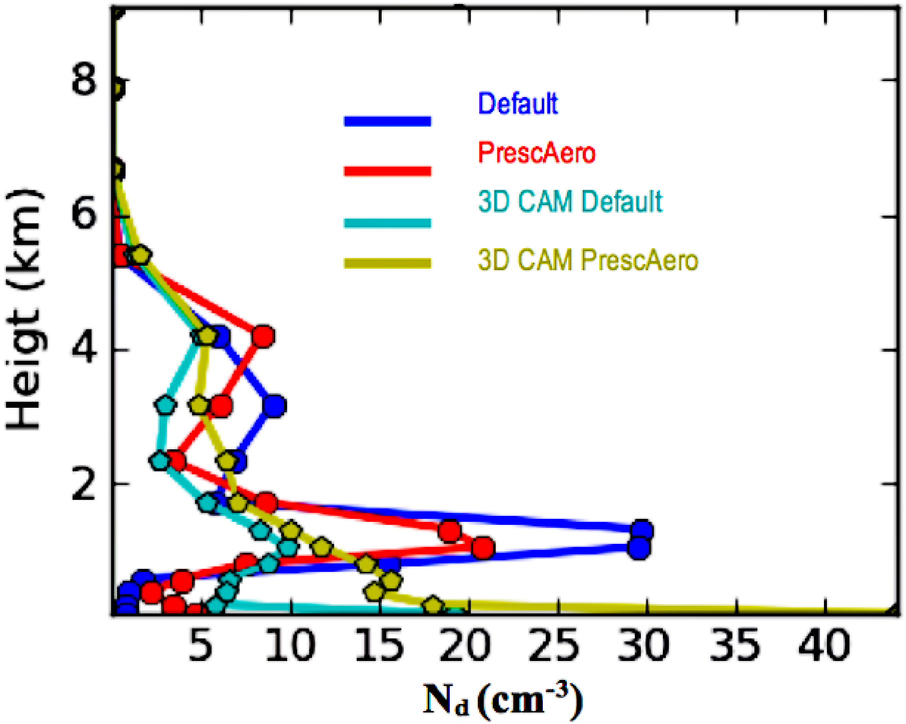

Figure 11. Profiles of in-cloud droplet number concentrations (N_d) during the ARM95 IOP period. Blue = Default case and Red = PrescAero case; Cyan = 10 years July average default global CAM extracted at the location of ARM95; Yellow = 10 years July average PrescAero global CAM extracted at the location of ARM95.

GMDD
7, 7693–7731, 2014

Aerosol specification in single-column CAM5

B. Lebassi-Habtezion and P. Caldwell